JOURNAL OF GEOPHYSICAL RESEARCH, VOL. 105, NO. A10, PAGES 22,979–22,989, OCTOBER 1, 2000

Electrodynamic coupling of high and low latitudes: Observations on May 27, 1993

A. T. Kobea,[1] A. D. Richmond,[2] B. A. Emery,[2] C. Peymirat,[3] H. Lühr,[4] T. Moretto,[5] M. Hairston,[6] and C. Amory-Mazaudier[7]

Abstract. The penetration of disturbance electric fields from the polar region to the magnetic equator on the dayside of the Earth is examined with geomagnetic data on May 27, 1993. First, we examine a dayside equatorial disturbance that followed the rapid recovery of magnetic activity from a storm and that has the characteristics of overshielding caused by persistent region-2 field-aligned currents. It lasted ~ 3 hours. Second, we analyze a series of fluctuations with periods of 25-75 min, to determine the variations of amplitude and phase with magnetic latitude and magnetic local time. The fluctuations were highly coherent at all latitudes between the magnetic equator and the auroral zone, but the coherency decreased in the polar cap. A northward fluctuation at the equator during midday hours accompanied auroral zone fluctuations that were southward before noon, eastward around noon, and northward after noon. The amplitudes decreased away from the auroral zone toward midlatitudes but were amplified under the equatorial electrojet. No detectable phase differences are found, indicating that any temporal lags which might be induced by persistence in the region-2 field-aligned currents are less than 1 min for fluctuations having periods like those examined here. A synoptic inversion analysis of the high-latitude magnetic data to estimate the time-varying high-latitude electric potential patterns shows that fluctuations of the high-latitude east-west potential gradient tended to be concentrated around midday, where they were in phase with fluctuations in the midday east-west potential gradient at the magnetic equator.

1. Introduction

A part of the geomagnetic disturbances observed nearly simultaneously over the globe [e.g., *Onwumechilli and Ogbuehi*, 1962] are attributed to magnetospheric electric fields and currents that connect to the high-latitude ionosphere and penetrate through the middle- and low-latitude ionosphere all the way to the equator [e.g., *Nishida et al.*, 1966; *Reddy et al.*, 1979; *Fejer et al.*, 1990a; *Gonzales et al.*, 1983; *Sibeck*, 1993; *Kikuchi et al.*, 1996; *Abdu et al.*, 1998; *Kobea et al.*, 1998]. Such geomagnetic disturbances generally fall off in amplitude from the auroral zone toward lower latitudes, but they exhibit an amplitude enhancement of about a factor of 4 near the magnetic equator on the dayside of the Earth, associated with modulation of the equatorial electrojet [e.g., *Nishida*, 1968; *Kikuchi et al.*, 1996]. This distinguishes them from disturbances in distant magnetospheric currents like the ring current, the Chapman-Ferraro current, and the magnetotail current that produce widespread magnetic perturbations on both the dayside and nightside of the Earth, without any enhancement under the equatorial electrojet.

To date, observational studies relating magnetic disturbances at high and low latitudes have not established any systematic temporal differences among the different locations. Studies by *Nishida et al.* [1966] and *Nishida* [1968, 1971] found that a type of disturbance called *DP* 2, associated with fluctuations in the north-south component of the interplanetary magnetic field, occurs nearly simultaneously at high and low lat-

[1]Laboratoire de Physique de l'Atmosphère, Abidjan, Côte d'Ivoire.
[2]High Altitude Observatory, National Center for Atmospheric Research, Boulder, Colorado.
[3]Centre d'Etude Spatiale des Rayonnements, Toulouse, France.
[4]Geoforschungszentrum Potsdam, Germany.
[5]Danish Space Research Institute, Copenhagen.
[6]Center for Space Science, University of Texas at Dallas, Richardson.
[7]Centre d'Etudes des Environnements Terrestres et Planétaries,
Observatoire de Saint-Maur, Saint-Maur-Des-Fossés, France.

Paper number 2000JA000058.
0148-0227/00/2000JA000058$09.00.

Table 1. Coordinates of Magnetometers Used in This Study

Code	Name	Geographic, deg		Quasi-Dipole, deg		Source
		Lat.	Long.	Lat.	Long.	
		Low-Latitude Stations				
EBR	Ebro	40.82	0.49	35.05	76.87	EBR
MOP	Mopti	14.50	-4.08	3.85	69.90	COC
KOU	Koutiala	12.36	-5.45	1.49	68.32	COC
NIE	Nielle	10.20	-5.64	-0.89	67.88	COC
		40° QD-Meridian High-Latitude Zone				
THL	Thule	77.48	290.83	85.46	34.20	DMI
SVS	Savissivik	76.02	294.90	83.71	36.46	DMI
UMQ	Umanaq	70.68	307.87	76.99	44.28	DMI
GDH	Godhavn	69.25	306.47	75.91	40.65	DMI
ATU	Attu	67.93	306.43	74.68	39.18	DMI
SKT	Sukkertoppen	65.42	307.10	72.17	37.85	DMI
GHB	Godthaab	64.17	308.27	70.74	38.39	DMI
FHB	Frederikshaab	62.00	310.32	68.20	39.48	DMI
NAQ	Narsarsuaq	61.18	314.57	66.50	43.77	DMI
STJ	St. Johns	47.60	307.32	54.14	31.10	WDC
		70° QD-Meridian High-Latitude Zone				
DMH	Danmarkshavn	76.77	341.37	77.14	87.47	DMI
MCG	MAGIC GISP	72.57	321.55	76.33	62.35	UMI
DNB	Daneborg	74.30	339.78	75.08	80.88	DMI
SCO	Scoresbysund	70.48	338.03	71.63	73.60	DMI
AMK	Ammassalik	65.60	322.37	69.42	54.73	DMI
LRV	Leirvogur	64.18	338.30	65.11	67.83	WDC
FAR	Faroes	62.05	352.98	60.70	78.19	SAM
LER	Lerwick	60.13	358.82	57.93	81.71	WDC
GML	Glenmore	57.16	356.32	54.85	78.30	SAM
ESK	Eskdalemuir	55.32	356.80	52.69	77.90	INT
		105° QD-Meridian High-Latitude Zone				
NRD	Nord	81.60	343.33	80.81	106.11	DMI
NAL	Ny Alesund	78.92	11.95	75.90	112.17	WDC
HOP	Hopen Island	76.51	25.01	72.74	116.01	IMG
BJN	Bear Island	74.50	19.20	71.18	109.10	IMG
SOR	Soroya	70.54	22.22	67.07	107.01	IMG
TRO	Tromso	69.66	18.94	66.38	103.74	WDC
KEV	Kevo	69.76	27.01	66.02	110.02	IMG
MAS	Masi	69.46	23.70	65.89	107.22	IMG
KIL	Kilpisjarvi	69.05	20.70	65.65	104.58	IMG
MUO	Muonio	68.02	23.53	64.45	105.99	IMG
KIR	Kiruna	67.83	20.42	64.43	103.43	WDC
SOD	Sodankyla	67.37	26.63	63.62	107.99	INT
PEL	Pello	66.90	24.08	63.27	105.66	IMG
OUL	Oulu	65.10	25.85	61.34	105.98	SAM
NOR	Nordli	64.37	13.36	61.29	95.58	SAM
OUJ	Oulujarvi	64.52	27.23	60.68	106.78	IMG
HAN	Hankasalmi	62.30	26.65	58.41	105.20	IMG
		105° QD-Meridian High-Latitude Zone (continued)				
NUR	Nurmijarvi	60.50	24.65	56.60	102.74	IMG
KVI	Kvistaberg	59.50	17.63	55.84	96.50	INT
LOV	Lovo	59.35	17.83	55.66	96.60	INT
BFE	Brorfelde	55.63	11.67	51.89	90.05	DMI
		Other High-Latitude Stations				
RBC	Resolute Bay	74.70	265.10	83.54	-42.57	WDC
MBC	Mould Bay	76.20	240.60	80.81	-88.40	INT

Table 1. (continued)

Code	Name	Geographic, deg Lat.	Geographic, deg Long.	Quasi-Dipole, deg Lat.	Quasi-Dipole, deg Long.	Source
CBB	Cambridge Bay	69.10	255.00	77.36	-52.85	WDC
BLC	Baker Lake	64.33	263.97	74.16	-33.80	WDC
CCS	Cape Chelyuskin	77.72	104.27	71.61	175.46	WDC
BRW	Barrow	71.30	203.25	69.77	-110.04	WDC
YKC	Yellowknife	62.43	245.50	69.48	-60.64	WDC
FCC	Fort Churchill	58.76	265.92	69.08	-28.67	WDC
FSP	Fort Simpson	61.76	238.77	67.44	-68.51	WDC
FYU	Fort Yukon	66.57	214.70	67.05	-96.32	WDC
PDB	Poste de la Baleine	55.27	282.22	65.99	-2.00	WDC
CMO	College	64.87	212.17	64.86	-97.05	WDC
CHD	Chokurdakh	70.62	149.89	64.54	-146.36	210
CWE	Cape Wellen	66.17	190.17	62.58	-114.91	WDC
MEA	Meanook	54.62	246.67	62.09	-55.03	WDC
AMU	Anchorage	61.24	210.13	60.79	-96.33	WDC
GLL	Glenlea	49.60	262.90	59.84	-31.61	WDC
SIT	Sitka	57.07	224.67	59.68	-80.72	WDC
POD	P. Tunguska	61.60	90.00	56.60	162.88	WDC
OTT	Ottawa	45.40	284.55	56.27	0.55	WDC
YAK	Yakutsk	62.08	129.67	55.88	-159.52	WDC
NEW	Newport	48.26	242.88	54.89	-57.27	WDC
VIC	Victoria	48.52	236.58	53.77	-64.46	WDC
MGD	Magadan	60.12	151.02	53.44	-141.20	210
ARS	Arti	56.43	58.57	51.83	131.91	WDC
NVS	Novosibirsk	55.03	82.90	50.15	155.48	WDC

Sources: EBR, Observatori de l'Ebre; COC, Université Cocody; DMI, Danish Meteorological Institute; WDC, World Data Center A; UMI, University of Michigan; SAM, SAMNET; INT, INTERMAGNET; IMG, IMAGE; 210, 210° Magnetic Meridian Project.

itudes to within a few minutes. *Kikuchi et al.* [1996] determined that the time delay of *DP* 2 and related disturbances between magnetic latitudes of 66° and the equator on the dayside is very short, at the most some tens of seconds. This is consistent with the induction timescale for the electric field to penetrate to the equator, of the order of seconds [*Vasyliunas*, 1972].

However, some theoretical models predict the possibility of significant temporal differences between disturbances at high latitudes and at middle and low latitudes. The manner in which the electric fields and currents penetrate from the polar cap through the auroral region into midlatitudes is affected by the redistribution of magnetospheric hot plasma that is the source of region-2 field-aligned currents into and out of the ionosphere [e.g., *Vasyliunas*, 1972; *Jaggi and Wolf*, 1973; *Southwood*, 1977; *Harel et al.*, 1981; *Senior and Blanc*, 1984; *Peymirat and Fontaine*, 1994; *Fejer*, 1997]. Under steady state conditions these region-2 currents would tend to minimize the penetration of ionospheric electric fields and currents between the auroral region and middle and low latitudes, producing a "shielding" effect [e.g., *Karlson*, 1963; *Block*, 1966; *Vasyliunas*, 1972; *Jaggi and Wolf*, 1973; *Southwood*, 1977]. On the other hand, during time-varying disturbances the distribution of magnetospheric plasma and the accompanying shielding currents may not have time to develop the appropriate balance for shielding, and there may exist either undershielding or overshielding, [e.g., *Vasyliunas*, 1972; *Jaggi and Wolf*, 1973; *Southwood*, 1977; *Kelley et al.*, 1979; *Gonzales et al.*, 1979, 1983; *Spiro et al.*, 1988; *Fejer et al.*, 1990b]. During either undershielding or overshielding, relatively strong disturbance electric fields can penetrate to the equator, with the direction of the fields tending to be reversed between the two cases. The overshielding represents the low-latitude electrical disturbance produced upon a rapid decrease of magnetospheric convection, and it is caused by temporary maintenance of the region-2 field-aligned currents generated by the hot magnetospheric plasma distribution that was established during the prior strong convection [e.g., *Kelley et al.*, 1979]. Westward perturbations of the dayside electric field have been observed in cases associated with a turning of the interplanetary magnetic field (IMF) from south to north [*Kelley et al.*, 1979; *Fejer et al.*, 1979]. The time delay associated with the reestablishment of shielding implies that temporal differences will be introduced between disturbances poleward and equatorward of the region-2 currents, so that polar and equatorial disturbances will not be strictly simultaneous.

In this paper we analyze observations of two types of disturbances in order to identify possible shielding/overshielding effects on the penetration of electric

fields from the polar region to the magnetic equator on the dayside of the Earth. The first event is the recovery from a storm disturbance, when overshielding might be anticipated. The second event is a series of fluctuations in the auroral and equatorial magnetic fields. An overview of these events was presented by *Kobea et al.* [1998]. A companion paper [*Peymirat et al.*, this issue] presents simulation results from a model of the coupled magnetosphere-ionosphere system, in order to study the shielding/overshielding mechanism as it relates to events of the types presented here.

2. Magnetometer Data

We use 1-min digital magnetometer data recorded at high, middle, and equatorial latitudes on May 27, 1993, during the International Equatorial Electrojet Year. Table 1 gives the coordinates of the magnetometers, and Figure 1 shows their locations in magnetic coordinates. Quasi-Dipole (QD) coordinates [*Richmond*, 1995] are used, referenced to an altitude of 110 km. Depending on the instrument, the measured horizontal components are either H (magnetic northward) and E (magnetic-eastward declination perturbation, in nanoteslas), or X (geographic northward) and Y (geographic eastward). *Kobea et al.* [1998] showed magnetograms for the equatorial station NIE and the midlatitude station EBR, as well as the X components from some of the Scandinavian International Monitor for Auroral Geomagnetic Effects (IMAGE) stations and the H components from the Greenland stations (except MCG) plus BFE. They also showed hourly data from additional sites and the hourly *Dst* index. In the present paper we analyze these data and additional data in more detail, to clarify the temporal relations among them in regard to the coupling of high and low latitudes.

For each station component the corresponding values on the magnetically quiet day May 25, 1993, are subtracted so that we can examine only the disturbance component. The horizontal components are additionally corrected for *Dst* effects. One-minute *Dst* values were generated from the standard hourly values by fitting parabolas over each hour, with beginning points midway between that hour's value and the previous hour's value, ending points midway between that hour's value and the next hour's value, and with an hourly averaged value equal to the original *Dst* value for that hour. The 1-min *Dst* values are multiplied by the cosine of the geomagnetic latitude and subtracted from the geomagnetic northward component at each station. The 1-min *Dst* values range from 51 nT (0130 UT) to -38 nT (0731 UT) and produce particularly important corrections at the middle- and low-latitude stations.

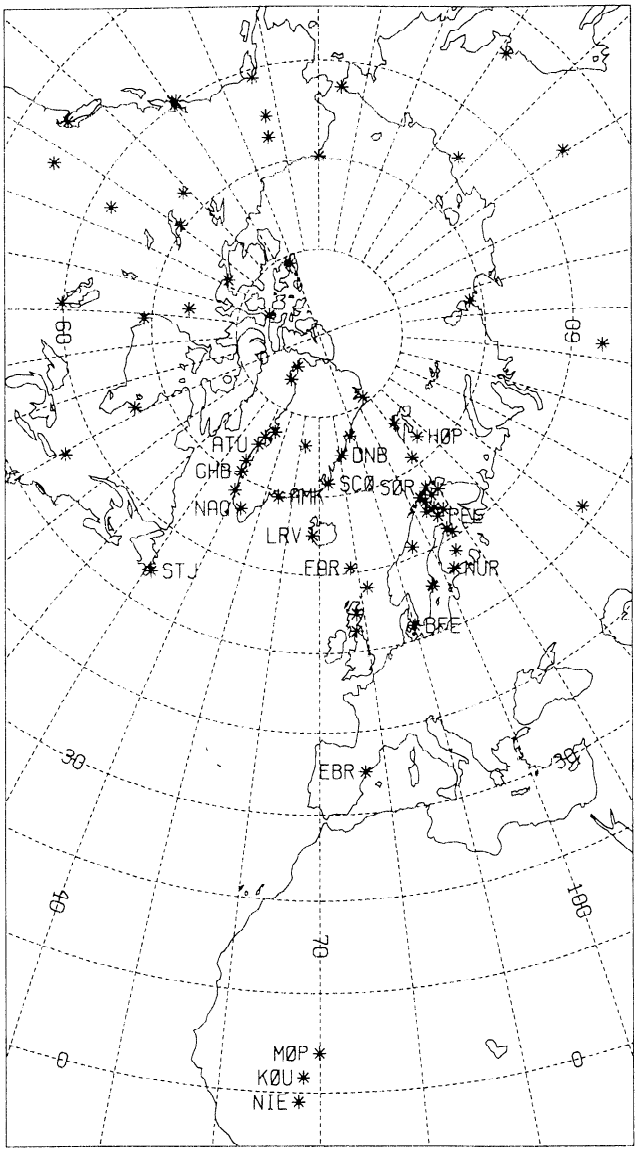

Figure 1. The locations of the magnetometers (stars) in magnetic (quasi-dipole) coordinates. Three-letter codes are shown only next to selected magnetometers.

3. Overshielding Event

Figure 2 shows 5-min averages of the auroral electrojet indices computed from the upper (AU) and lower (AL) envelopes of superposed H perturbations from all magnetometers lying between 55° and 76° magnetic latitude, during the time interval 3 – 15 UT. Also shown in Figure 2 are the 1-min H data for three magnetometers near the 70° magnetic longitude: two auroral stations (SCO, 72° magnetic latitude, and LRV, 65°) and the magnetic-equatorial station NIE (-1°). (The two auroral stations contribute to the AU and AL indices.) For these three stations, magnetic local time is similar to universal time. Note that the scale for NIE has been amplified by a factor of 4. The AU and AL indices show that strong eastward and westward electrojets were present in the auroral zone between ~ 0400 and 0800 UT. LRV was under the westward electrojet. The westward electrojet was equatorward of SCO until ~ 0600 UT but moved northward to be partly over SCO between 0600 and 0800 UT.

The interesting thing to note in Figure 2 is that the NIE trace began to decrease around 0730 UT, just about the time that the high-latitude magnetic activity seen in the *AU* and *AL* indices started to subside rapidly. The decrease in magnitude of the *AU* and *AL* indices at this time suggests that the cross polar cap electric potential probably also dropped rapidly. Indeed, the cross polar cap potentials observed by the polar-orbiting Defense Meteorological Satellite Program (DMSP) F8 and F11 spacecraft, processed as described by *Hairston et al.* [1998] and listed in Table 2, show that the potential decreased from ~ 104 kV at 0738 UT to ~ 66 kV at 0829 UT. The DMSP estimates of potential require a complete overpass of either the northern or the southern magnetic polar region, and they are unfortunately not sufficiently frequent to determine the detailed time variation of the cross polar cap potential.

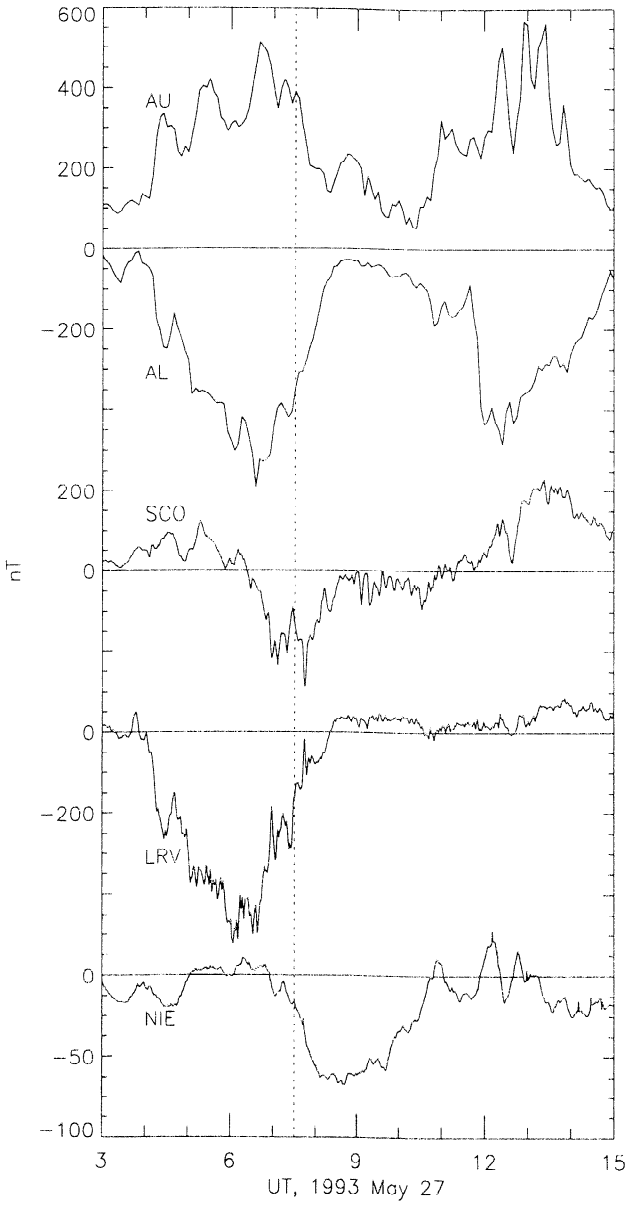

Figure 2. *AU* and *AL* indices and disturbance variations of the *H* component of the Earth's magnetic field at SCO, LRV, and NIE on May 27, 1993. *Dst* and quiet day variations have been subtracted. The vertical scale for the variation at NIE is magnified by a factor of 4. Magnetic local time (MLT) is similar to UT for SCO, LRV, and NIE. The vertical dotted line at 0730 UT shows approximately the time at which auroral magnetic activity began a rapid decrease and the time at which a large negative perturbation at NIE began.

At NIE the negative excursion which started at ~ 0730 UT reached −65 nT at ~ 0800 UT. It remained around that level for a while before recovering between ~ 0930 and 1030 UT. Hourly data presented by *Kobea et al.* [1998] at various equatorial locations (their Figure 2) show that the *H* perturbations were much stronger at NIE and KOU than at MOP, characteristic of the equatorial electrojet enhancement of ionospheric currents within a few degrees of the magnetic equator. The negative H excursion between 0730 and 1030 UT is indicative of a westward perturbation in the equatorial electric field that drives the equatorial electrojet. *Kobea et al.* showed that it was sufficiently strong to reverse the eastward electrojet that normally occurs on quiet days and to cause a cessation in electrojet plasma irregularities between 0800 and 0950 UT measured by the Korhogo radar in the same sector as NIE. This negative excursion appears to constitute a prompt equatorial response to the large decrease in the high-latitude convection, as a result of overshielding.

4. Magnetic Fluctuation Event

Between 1000 and 1400 UT, several large-amplitude fluctuations in the magnetic variations are apparent in many of the magnetometer traces, as, for example, in the *H* trace for NIE in Figure 2. At SCO and LRV, the fluctuations are primarily in the *E* component, as discussed in section 4.1, and are relatively weak in the *H* traces shown in Figure 2. These fluctuations offer the opportunity to examine relations between disturbances in the auroral oval and at low latitudes.

Table 2. Polar Cap Potential Drops Estimated From DMSP Overpasses

Time, UT	Potential, kV
0414	87
0505	95
0556	101
0647	121
0738	104
0829	66
0833	62
1106	105
1157	87
1248	99
1339	100

DMSP, Defense Meteorological Satellite Program.

4.1. Spatial Coherence of the Oscillations

Figure 3 shows plots of magnetic variations between 1000 and 1400 UT for several locations, where the data have been high-pass-filtered by removal of a 2-hour running mean. This filter multiplies the amplitude of a wave of period T by the factor

$$1 - \left(\frac{T}{2\pi \mathrm{hr}}\right) \sin\left(\frac{2\pi \mathrm{hr}}{T}\right), \qquad (1)$$

which deviates from 1.0 by at most 19% for the waves under consideration, that is, for $T \leq 75$ min, but becomes small for wave periods longer than several hours. Figures 3a and 3b are plots of high-latitude variations for two meridional chains on either side of the 70° magnetic meridian: Figure 3a shows the H component for magnetometers near the 40° magnetic meridian, from 75° magnetic latitude (ATU) to 54° (STJ) in the western Greenland zone, and Figure 3b shows the X component for magnetometers near the 105° magnetic meridian, from 73° magnetic latitude (HOP) to 57° (NUR), in the Scandinavian zone. (Since the magnetic declination is only 5°–7.5° for the Scandinavian sites, there is not much difference between X and H.) Only selected magnetometers are shown for each chain. Figures 3c and 3d show variations near the 70° magnetic meridian: Figure 3c shows the E component for high-latitude magnetometers running from 75° magnetic latitude (DNB) to 61° (FAR), and Figure 3d shows the H component for middle- and low-latitude magnetometers, from 35° magnetic latitude (EBR) to -1° (NIE).

Fluctuations with periods of ~ 25 to 75 min are present at all the stations, although they are weak at the midlatitude station EBR. The vertical dashed lines are placed near maxima in the low-latitude traces, occurring around 1054, 1210, 1246, 1310, and 1352 UT. For magnetic latitudes between the equator and ~ 70°, that is, up to GHB, SOR, and SCO in Figures 3a-3c, the fluctuations are strongly correlated, with no detectable phase differences that exceed the 1-min resolution of

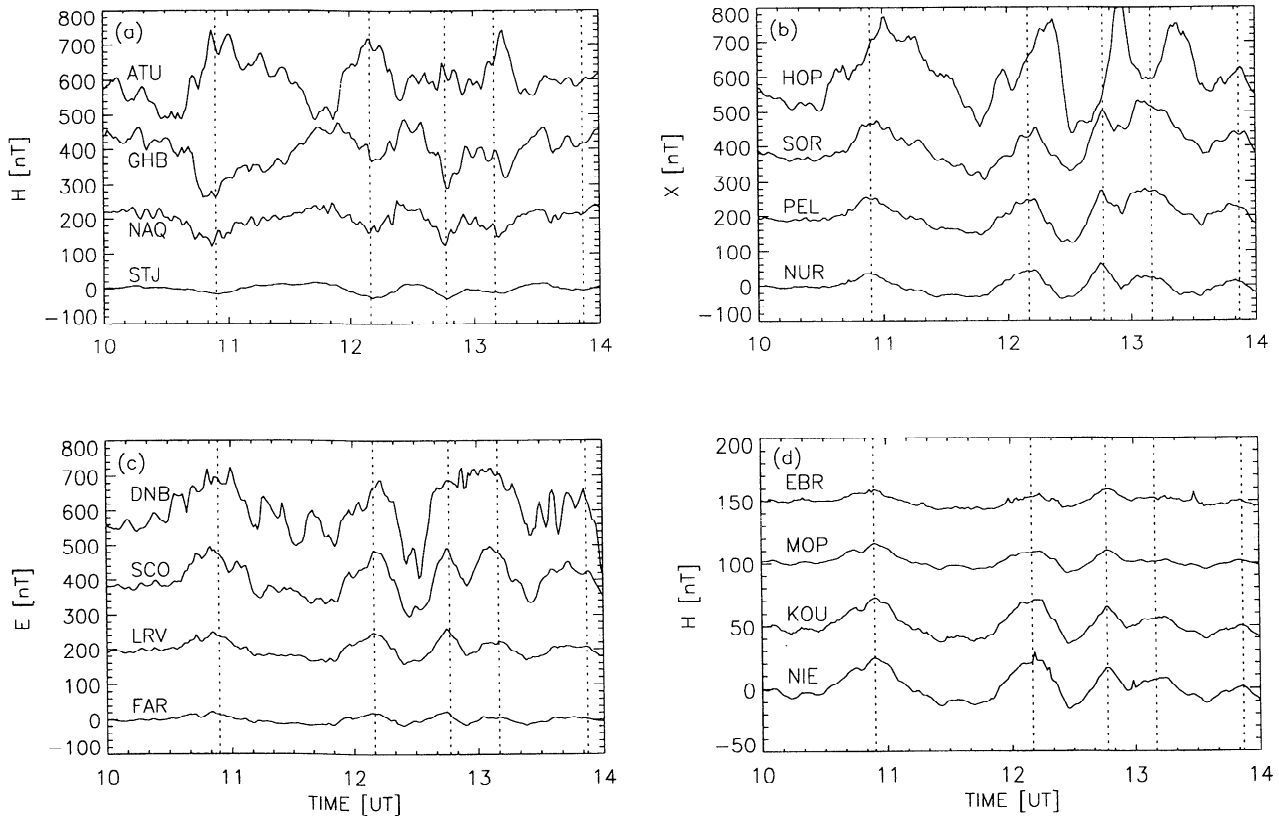

Figure 3. Magnetic field fluctuations observed in the time interval 1000–1400 UT on May 27, 1993, for selected stations. A 2-hour running mean has been subtracted. (a) H component for magnetometers near the 40° magnetic meridian, from 75° magnetic latitude (ATU) to 54° (STJ). For STJ the H values were computed from the recorded X and Y values. Successive traces have been shifted upward in increments of 200 nT. (b) X component for magnetometers near the 105° magnetic meridian, from 73° magnetic latitude (HOP) to 57° (NUR). Successive traces have been shifted upward in increments of 200 nT. (c) E component for magnetometers near the 70° magnetic meridian, from 75° magnetic latitude (DNB) to 61° (FAR). Successive traces have been shifted upward in increments of 200 nT. (d) H component for magnetometers near the 70° magnetic meridian, from 35° magnetic latitude (EBR) to -1° (NIE). Successive traces have been shifted upward in increments of 50 nT.

our data. At higher latitudes the features of the fluctuations start to change, more so for the north-south perturbations (H and X) than for the east-west perturbations (E). The low-latitude H variations (Figure 3d) are negatively correlated with the northward variations up to 70° magnetic latitude in the western Greenland zone (Figure 3a), but they are positively correlated with those up to 70° latitude in the Scandinavian zone (Figure 3b). The meridian of the transition between in-phase and out-of-phase northward fluctuations appears to lie near 70° magnetic longitude, since the fluctuations in H at SCO and LRV (Figure 2) are relatively small, although their E fluctuations are large. The correlation between the equatorial fluctuations and those in the Scandinavian zone is particularly strong: typical correlation coefficients of around 0.90 are found between the high-pass-filtered variations for this 4-hour period at the Scandinavian zone stations up to 70° and the equatorial stations MOP and NIE. Above 71° magnetic latitude the correlations decrease, and the variations tend to have noticeable phase shifts with respect to those at the lower latitudes. The lack of noticeable phase differences between the equator and 70° is consistent with the work of *Kikuchi et al.* [1996], who examined a different event.

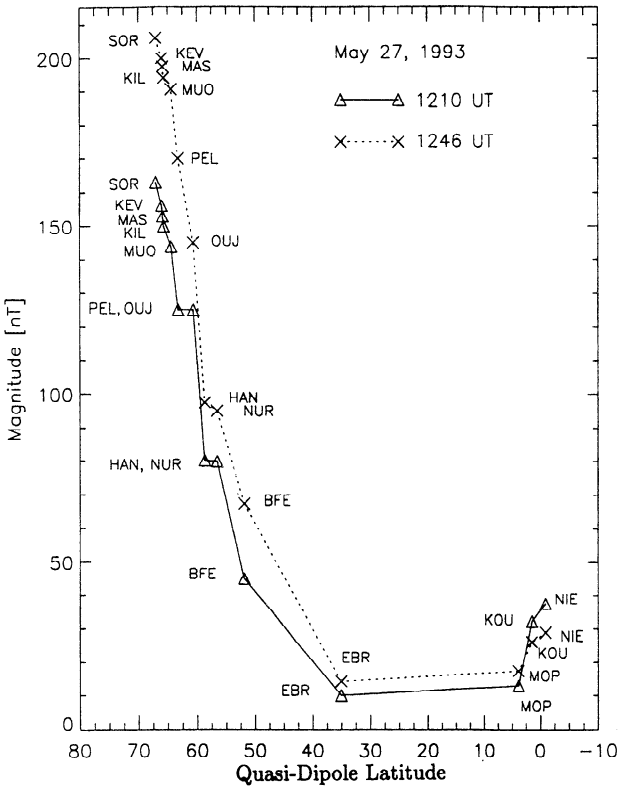

Figure 4. Latitudinal profile of the fluctuations at 1210 and 1246 UT extending to the equator, in the longitudinal sector ranging from 65° to 120° magnetic longitude including IMAGE and the West African network.

4.2. Latitudinal Profile of the Fluctuation Amplitude

In this section the study of the latitudinal profile of the fluctuation event indicates the degree of attenuation of the electric field away from the high-latitude source. *Kikuchi et al.* [1996] examined the latitude variation of DP 2 fluctuation amplitudes between the IMAGE stations and equatorial stations in the Brazilian and central African sectors. They found a rapid falloff in amplitude with decreasing latitude away from the auroral zone, until near the equator where the amplitude increased under the equatorial electrojet with an enhancement ratio of 3 in central Africa and 4 in Brazil. *Reddy et al.* [1979] concluded tentatively that auroral and polar latitude electric field perturbations penetrate to the equatorial latitude with a reduction factor of about a few tens applicable to the longitude sector of the source region. Figure 4 shows the latitudinal profile of the fluctuations at 1210 and 1246 UT extending to the equator, in the magnetic longitude sector ranging from 65° to 120° including the West African network and the IMAGE stations. Note that we measure the magnitude from the value obtained by connecting the minima of the fluctuations in the original (unfiltered) data around 1130 and 1230 UT, respectively, to the maxima at 1210 and 1246 UT. There is a monotonic decrease of the amplitude with decreasing latitude down to EBR and then a slight increase between EBR and MOP, with a substantial enhancement at the stations KOU and NIE under the direct influence of the equatorial electrojet. For instance, at 1210 UT the magnitude reached successively 163 nT at SOR, 45 nT at BFE, and 10 nT at EBR, but it increased appreciably to reach 37.5 nT at NIE, approaching nearly the amplitude at BFE. Similar equatorial enhancements of DP 2 have been pointed out by *Nishida et al.* [1966], *Nishida* [1968, 1971], and *Kikuchi et al.* [1996], and these enhancements confirm that the main source of the low-latitude magnetic variations is due to currents in the ionosphere rather than the distant magnetosphere.

4.3. Synoptic Characteristics of the Dayside High-Latitude Electrodynamics

To synthesize the high-latitude data, we use them as inputs to the Assimilative Mapping of Ionospheric Electrodynamics (AMIE) procedure [*Richmond and Kamide*, 1988]. This allows us to estimate the patterns of equivalent current and ionospheric electric potential above 50° magnetic latitude. The conductances are dominated by solar illumination, but we also include an auroral contribution estimated from the model of *Fuller-Rowell and Evans* [1987], with modifications in regions near magnetometers, using the formulas of *Ahn et al.* [1998]. The statistical background model of electric potential, which is modified by AMIE, is that of *Foster et al.* [1986]. Five-minute averages of the data are used, in order to smooth out rapid fluctuations that tend to represent very localized features.

Figure 5 shows two examples for different phases of the fluctuation, at 1230 and 1245 UT. On the left are the input data to AMIE above 50° magnetic latitude. In the middle are the estimated electric potentials. On the right are the estimated field-aligned current densities at the top of the ionosphere. In each pattern, noon magnetic local time (MLT) is toward the top. Because data are sparse in the 1600-2400 and 0700-1000 MLT sectors, the patterns in these sectors should be interpreted with caution. The patterns of equivalent current function (not shown) are very similar to those for the electric potential. The fluctuations of interest in this paper appear primarily on the dayside, and so we shall ignore the pattern on the nightside, where, as it happens, there was a substorm in its recovery phase (see the *AL* index in Figure 2).

The strong negative potential that minimizes in the polar cap on the dayside is characteristic of an IMF with a large, positive B_y component [e.g., *Weimer*, 1995]. At 1230 UT the potential minimum lies at noon, but it shifts to the afternoon by 1245 UT, while the region of positive potential penetrates toward noon around 72° magnetic latitude. The downward field-aligned currents that maximize around 65° in the afternoon are characteristic of region-2 currents that normally flow in the central and equatorward portions of the auroral oval. Region-1 currents, which tend to lie at or near the polar cap boundary, are not always clearly defined in Figure 5 but appear to be centered generally around 72°-75° magnetic latitude on the dayside.

In order to show more clearly the potential changes associated with the fluctuations, Figure 6 plots the po-

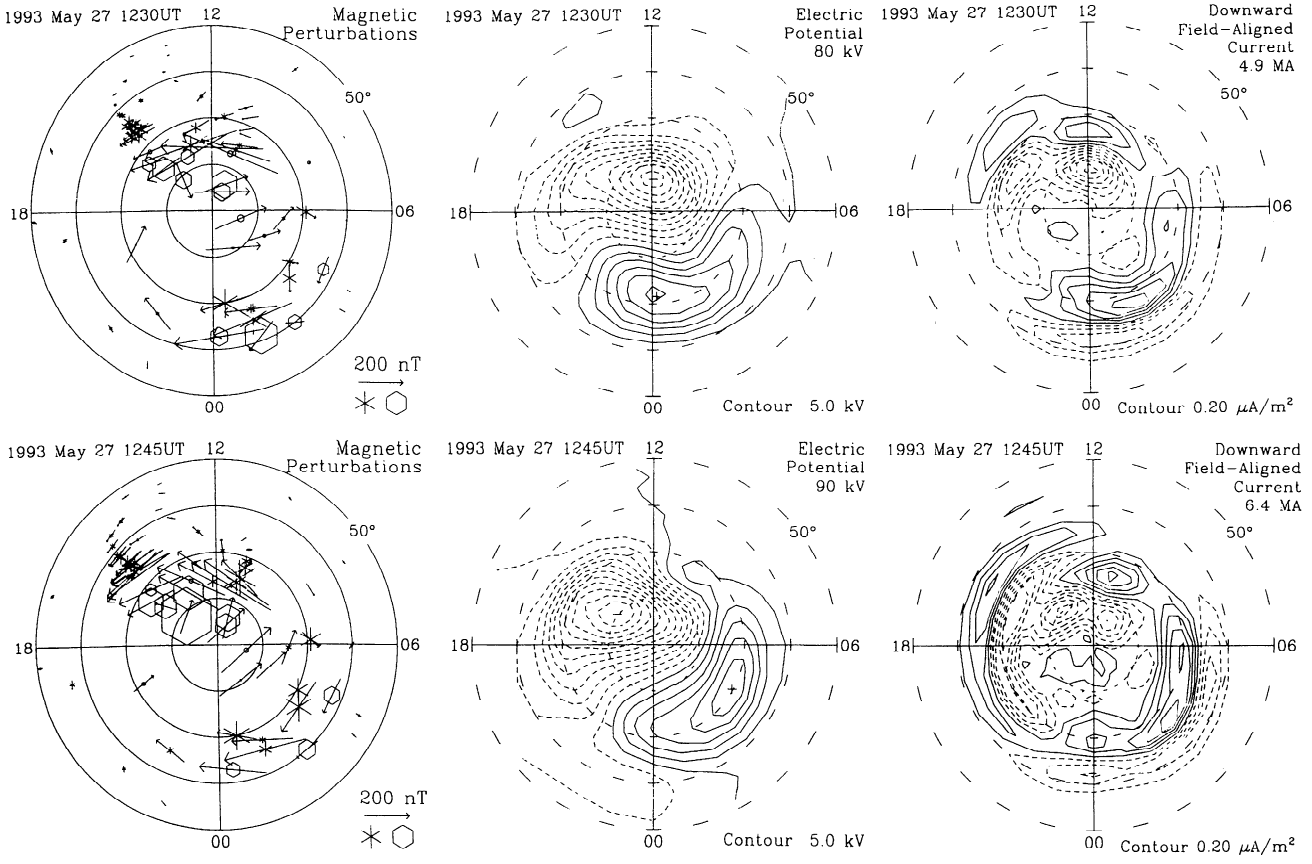

Figure 5. (left) Observed magnetic perturbations, (middle) estimated electric potentials, and (right) estimated field-aligned current density at the top of the ionosphere at 1230 UT (top) and 1245 UT (bottom) on May 27, 1993. Coordinates are magnetic latitude, from 50° to the north magnetic pole, and magnetic local time. The observed horizontal magnetic perturbations are shown by arrows that are rotated 90° clockwise in order to illustrate the direction of overhead equivalent current. The vertical magnetic perturbations are shown by stars (downward) or hexagons (upward). The scales corresponding to 200 nT are shown at the bottom. The electric-potential contour interval is 5 kV, with negative potentials indicated by dashed lines. The maximum and minimum potentials are shown by a plus and minus, respectively, with the total potential difference given at the upper right. Downward field-aligned currents are shown by solid contours, and upward currents are shown by dashed contours. The contour interval is 0.2 $\mu A/m^2$, starting at ± 0.1 $\mu A/m^2$. The hemispheric integral of the total downward current density is given at the upper right.

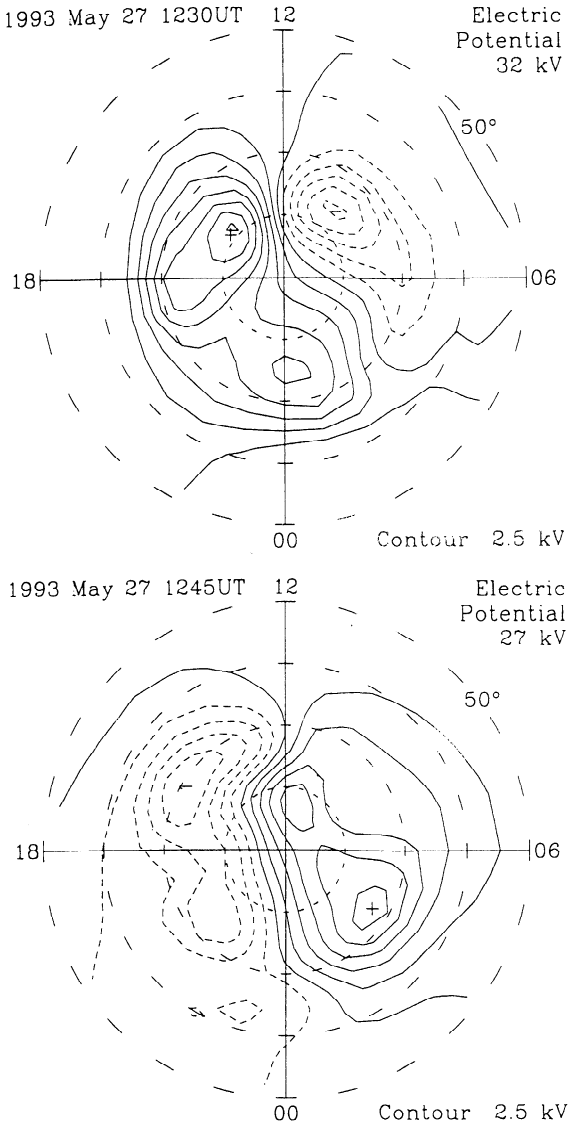

Figure 6. Electric potentials at 1230 and 1245 UT on May 27, 1993, with a 2-hour running mean subtracted to emphasize the fluctuations. The contour interval is 2.5 kV.

tentials with a 2-hour running mean subtracted. As in our high-pass filtering of the data shown in Figure 3, this brings out the fluctuating component. However, the filtering here is done in the nonrotating magnetic-latitude/MLT reference frame, not in the rotating reference frame of the Earth. Focusing on the dayside, we see that the fluctuations in the eastward electric field at the dayside polar cap boundary, that is, the fluctuations in the westward gradient of the potential at 72°-75° magnetic latitude, tend to be concentrated around the noon meridian.

As the high-latitude potential fluctuated during this 4-hour period, the direction of the morning-afternoon potential difference for the fluctuating component (i.e., with the 2-hour running mean removed) was in the same sense as that at the equator, as we infer by making the reasonable assumption that a positive H perturbation at the equator is created by an eastward ionospheric electric field that drives an eastward electrojet current. This indicates that the fluctuations in the morning-afternoon potential difference extended all the way from the polar region to the magnetic equator.

5. Discussion and Conclusions

By analyzing dayside magnetic variations at high and low latitudes during different types of magnetic disturbances on May 27, 1993, we have been able to clarify certain aspects of the penetration of electric fields and currents from the polar region to the magnetic equator. Following the rapid decline of auroral magnetic activity at the end of a magnetic storm, a strong westward perturbation of the equatorial electrojet appeared in the morning sector, which had characteristics that can be associated with overshielding. It lasted $\sim$ 3 hours.

Dayside magnetic fluctuations with periods of 25-75 min are found to be highly coherent at all latitudes between the magnetic equator and the auroral zone, with no detectable phase differences. For equatorial fluctuations that were northward, the auroral zone magnetic fluctuations tended to be southward before noon, eastward around noon, and northward after noon. The amplitudes decreased away from the auroral zone toward midlatitudes but were amplified under the equatorial electrojet. Although we might have expected some phase differences to occur, associated with shielding/overshielding effects due to the persistence of region-2 currents, any such differences that might exist were less than $\sim$ 1 min for the present event. Our application of the AMIE procedure to the dense regional array of magnetic data over the midday northern polar region, together with more widely spread data over the remainder of the polar region, has shown that the fluctuations of the high-latitude east-west potential gradient between 1000 and 1400 UT tended to be concentrated around midday. The direction of the high-latitude fluctuating morning-afternoon potential difference was the same as that for the fluctuating morning-afternoon potential difference at the equator that can be inferred from the fluctuations in the equatorial electrojet.

These observations of overshielding and of the penetration of fluctuating high-latitude electric fields to the equator have motivated us to use a numerical simulation model of magnetosphere-ionosphere coupling to investigate these effects further. The results of the simulation study are presented by *Peymirat et al.* [this issue].

Acknowledgments. We gratefully acknowledge the contributions of Jacques Vassal in the collection and processing of the African magnetometer data, and to E. Friis-Christensen, N. Olsen, and P. Stauning for assisting with the data from the Danish Meteorological Institute. We are indebted to the many organizations that contribute magnetometer data to the World Data Centers, and we acknowledge the National Geophysical Data Center (WDC-A) for

making these data available. We thank I. R. Mann and D. K. Milling for the SAMNET data. SAMNET is a PPARC National Facility deployed and operated by the University of York. We thank J.-J. Curto for the EBR data and C. R. Clauer for the MCG data. We would like to acknowledge the use of the 210° Magnetic Meridian (MM) data [*Yumoto et al.*, 1996], including CHD data provided by S. I. Solovyev and G. F. Krymsky of the Institute of Cosmophysical Research and Aeronomy and by V. A. Pilipenko of the Institute of the Physics of Earth, and including MGD data provided by E. F. Vershinin, V. V. Bogdaroj, and A. V. Buzevich of the Institute of Space Research and Radiowaves. The PI K. Yumoto manages the 210° MM observations project and group. The database is located at the Solar-Terrestrial Environment Laboratory (STEL) at Nagoya University. We also gratefully acknowledge the INTERMAGNET project for additional magnetometer data. We thank Gang Lu for helpful comments on a draft of this paper. This study was supported in part by NASA award W-17,384.

Janet G. Luhmann thanks the referees for their assistance in evaluating this paper.

References

Abdu, M. A., J. H. Sastri, H. Lühr, H. Tachihara, T. Kitamura, N. B. Trivedi, and J. H. A. Sobral, DP 2 electric field fluctuations in the dusk-time dip equatorial ionosphere, *Geophys. Res. Lett., 25*, 1511-1514, 1998.

Ahn, B.-H., A. D. Richmond, Y. Kamide, H. W. Kroehl, B. A. Emery, O. de la Beaujardière, and S.-I. Akasofu, An ionospheric conductance model based on ground magnetic disturbance data, *J. Geophys. Res., 103*, 14,769-14,780, 1998.

Block, L. P., On the distribution of electric fields in the magnetosphere, *J. Geophys. Res., 71*, 855-864, 1966.

Fejer, B. G., The electrodynamics of low-latitude ionosphere: Recent results and future challenges, *J. Atmos. Terr. Phys., 59*, 1465-1482, 1997.

Fejer, B. G., C. A. Gonzales, D. T. Farley, M. C. Kelley, and R. F. Woodman, Equatorial electric fields during magnetically disturbed conditions, 1, The effect of the interplanetary magnetic field, *J. Geophys. Res., 84*, 5797-5802, 1979.

Fejer, B. G., *et al.*, Low- and mid-latitude ionospheric electric fields during the January 1984 GISMOS campaign, *J. Geophys. Res., 95*, 2367-2377, 1990a.

Fejer, B. G., R. W. Spiro, R. A. Wolf, and J. C. Foster, Latitudinal variation of perturbation electric fields during magnetically disturbed periods: 1988 SUNDIAL observations and model results, *Ann. Geophys., 8*, 441-454, 1990b.

Foster. J. C., J. M. Holt, R. G. Musgrove, and D. S. Evans, Ionospheric convection associated with discrete levels of particle precipitation, *Geophys. Res. Lett., 13*, 656-659, 1986.

Fuller-Rowell, T., and D. S. Evans, Height-integrated Pedersen and Hall conductivity patterns inferred from the TIROS-NOAA satellite data, *J. Geophys. Res., 92*, 7606-7618, 1987.

Gonzales, C. A., M. C. Kelley, B. G. Fejer, J. F. Vickrey, and R. F. Woodman, Equatorial electric fields during magnetically disturbed periods, 2, Implications of simultaneous auroral and equatorial measurements, *J. Geophys. Res., 84*, 5803-5812, 1979.

Gonzales, C. A., M. C. Kelley, R. A. Behnke, J. F. Vickrey, R. Wand, and J. Holt, On the latitudinal variations of the ionospheric electric field during magnetospheric disturbances, *J. Geophys. Res., 88*, 9135-9144, 1983.

Hairston, M. R., R. A. Heelis, and F. J. Rich, Analysis of the ionospheric cross polar cap potential drop using DMSP data during the National Space Weather Program study period, *J. Geophys. Res., 103*, 26,337-26,347, 1998.

Harel, M., R. A. Wolf, P. H. Reiff, R. W. Spiro, W. J. Burke, F. J. Rich, and M. Smiddy, Quantitative simulation of a magnetospheric substorm, 1, Model logic and overview, *J. Geophys. Res., 86*, 2217-2241, 1981.

Jaggi, R. K., and R. A. Wolf, Self-consistent calculation of the motion of a sheet of ions in the magnetosphere, *J. Geophys. Res., 78*, 2852-2866, 1973.

Karlson, E. T., Streaming of a plasma through a magnetic dipole field, *Phys. Fluids, 6*, 708-722, 1963.

Kelley, M. C., B. G. Fejer, and C. A. Gonzales, An explanation for anomalous equatorial ionospheric electric fields associated with a northward turning of the interplanetary magnetic field, *Geophys. Res. Lett., 6*, 301-304, 1979.

Kikuchi, T., H. Lühr, T. Kitamura, O. Saka, and K. Schlegel, Direct penetration of the polar electric field to the equator during a DP2 event as detected by the auroral and equatorial magnetometer chains and the EISCAT radar, *J. Geophys. Res., 101*, 17,161-17,173, 1996.

Kobea, A. T., C. A. Mazaudier, J. M. Do, H. Lühr, E. Houngninou, J. Vassal, E. Blanc, and J. J. Curto, Equatorial electrojet as part of the global circuit: A case study from the IEEY, *Ann. Geophys., 16*, 698-710, 1998.

Nishida, A., Geomagnetic DP2 fluctuations and associated magnetospheric phenomena, *J. Geophys. Res., 73*, 1795-1803, 1968.

Nishida, A., DP 2 and polar substorm, *Planet. Space Sci., 19*, 205-221, 1971.

Nishida, A., N. Iwasaki, and T. Nagata, The origin of fluctuations in the equatorial electrojet: A new type of geomagnetic variations, *Ann. Geophys., 22*, 478-485, 1966.

Onwumechilli, A., and P. O. Ogbuehi, Fluctuations in the geomagnetic horizontal field, *J. Atmos. Terr. Phys., 24*, 173-190, 1962.

Peymirat, C., and D. Fontaine, Numerical simulation of magnetospheric convection including the effect of field-aligned currents and electron precipitation, *J. Geophys. Res., 99*, 11,155-11,176, 1994.

Peymirat, C., A. D. Richmond, and A. Kobea Toka, Electrodynamic coupling of high and low latitudes: Simulations of shielding/overshielding effects, *J. Geophys. Res.*, this issue.

Reddy, C. A., V. V. Somayajulu, and C. V. Devasia, Global-scale electrodynamic coupling of the auroral and equatorial dynamo regions, *J. Atmos. Terr. Phys., 41*, 189-201, 1979.

Richmond, A. D., Ionospheric electrodynamics using Magnetic Apex Coordinates, *J. Geomagn. Geoelectr., 47*, 191-212, 1995.

Richmond, A. D., and Y. Kamide, Mapping electrodynamic features of the high-latitude ionosphere from localized observations: Technique, *J. Geophys. Res., 93*, 5741-5759, 1988.

Senior, C., and M. Blanc, On the control of magnetospheric convection by the spatial distribution of ionospheric conductivities, *J. Geophys. Res., 89*, 261-284, 1984.

Sibeck, D. G., Transient magnetic field signatures at high latitudes, *J. Geophys. Res., 98*, 243-256, 1993.

Southwood, D. J., The role of hot plasma in magnetospheric convection, *J. Geophys. Res., 82*, 5512-5520, 1977.

Spiro, R. W., R. A. Wolf, and B. G. Fejer, Penetration of high-latitude-electric-field effects to low latitude during SUNDIAL 1984, *Ann. Geophys., 6*, 39-50, 1988.

Vasyliunas, V. M., The interrelationship of magnetospheric processes, in *Earth's Magnetosphere Processes*, edited by B. M. McCormac, pp. 29-38, D. Reidel, Norwell, Mass., 1972.

Weimer, D. R., Models of high-latitude electric potentials derived with a least-error fit of spherical harmonic coefficients, *J. Geophys. Res., 100*, 19,595-19,607, 1995.

Yumoto, K., and the 210° MM Magnetic Observation Group, The STEP 210° magnetic meridian network project, *J. Geomagn. Geoelectro., 48*, 1297-1309, 1996.

C. Amory-Mazaudier, Centre d'Etudes des Environnements Terrestres et Planétaires, Observatoire de Saint-Maur, 4 avenue de Neptune, F-94107 Saint-Maur-des-Fossés, France. (Christine.MAZAUDIER@cetp.ipsl.fr)

B. A. Emery and A. D. Richmond, High Altitude Observatory, National Center for Atmospheric Research, 3450 Mitchell Lane, Boulder, CO 80301. (emery@ucar.edu; richmond@ucar.edu)

M. Hairston, Center for Space Science, Mail Stop F022, University of Texas at Dallas, POB 830688, Richardson, TX 75083-0688. (hairston@utdallas.edu)

A. T. Kobea, Laboratoire de Physique de l'Atmosphère, 22 B. P. 582 Abidjan 22, Côte d'Ivoire. (kobeat@ci.refer.org)

H. Lühr, Geoforschungszentrum, Telegrafenberg, 14473 Potsdam, Germany. (hluehr@gfz-potsdam.de)

T. Moretto, Danish Space Research Institute, Juliane Maries Vej 30, DK-2100 Copenhagen, Denmark. (moretto@dsri.dk)

C. Peymirat, Centre d'Etude Spatiale des Rayonnements, 9 Avenue du Colonel Roche, 31028 Toulouse Cedex 4, France. (Christophe.Peymirat@cesr.fr)

(Received February 23, 2000; revised May 11, 2000; accepted May 11, 2000.)